Available online at www.sciencedirect.com
SCIENCE DIRECT
Polymer 47 (2006) 3229–3239
polymer
www.elsevier.com/locate/polymer

Theoretical investigations on the modulation of the polymer electronic and optical properties by introduction of phenoxazine

Li Yang [a], Ji-Kang Feng [a,b,*], Ai-Min Ren [a], Chia-Chung Sun [a]

[a] State Key Laboratory of Theoretical and Computational Chemistry, Institute of Theoretical Chemistry, Jilin University, Changchun 130023, China
[b] College of Chemistry, Jilin University, Changchun 130023, China

Received 18 December 2005; received in revised form 24 February 2006; accepted 27 February 2006
Available online 22 March 2006

Abstract

The color purity and efficiency of polyfluorene-based blue-emitting polymers is often compromised by long wavelengths, green emission bands and the charge injection difficulties. The incorporation of the phenoxazine units has been proved to significantly enhance the hole injection and charge carrier balance and at the same time efficiently suppress the keto defect emission. In this contribution, we apply quantum-chemical techniques to investigate poly(10-methylphenoxazine-3,7-diyl) (PPOZ) and its fluorene copolymer poly[(10-methylphenoxazine-3,7-diyl)-*alt*-2,7-(9,9-dimethyl-fluorene)] (PFPOZ), and gain a detailed understanding the influence of phenoxazine units on the electronic and optical properties of fluorene derivatives. The outcomes show that the highly non-planar conformation of phenoxazine ring in the ground state preclude sufficiently close intermolecular interactions essential to forming aggregates or excimers. Furthermore, the HOMO energies lift about 0.6 eV and thus the IPs decrease about 0.6 eV in PFPOZ, suggesting the significant improved hole-accepting and transporting abilities, due to the electron-donating properties of phenoxazine ring, which results in the enhanced performances in both efficiency and brightness compared with pristine polyfluorene.

Keywords: Fluorene; Phenoxazine; DFT

1. Introduction

Conjugated polymers have attracted much scientific and technological research interest during the past few decades because of their potential use as semiconductors and electroactive materials in diverse applications such as transistors, photovoltaic devices, non-linear optical devices, and polymer light-emitting diodes (PLEDs) [1]. In particular, interest in PLEDs fabricated from conjugated polymers has increased because such PLEDs have properties that are well-suited to flat panel displays: good processability, low-operating voltages, fast response times, and facile color tenability over the full visible range [2]. Synthesis and investigation of new conjugated polymers are essential to improving the electronic and optoelectronic properties of these materials and in turn improvement of the performance of the devices.

Polyfluorenes [3], which constitute an important class of π-conjugated organic materials because of their excellent chemical, thermal, and photochemical stabilities as well as the ease of structural tuning to adjust the electronic and morphological properties, have been extensively investigated and explored for various functional properties including electroluminescence and liquid crystalline and two-photon absorption properties for optoelectronic and photonic applications in the past few years. In addition to excellent luminescent properties, one general challenge in the field is achievement of high-electron affinity (n-type) conjugated polymers for improving electron injection/transport and low-ionization potential (p-type) conjugated polymers for better hole injection/transport in polymer electronic devices. Thus, many ways have been used to modulate the ionization potential (IP) and electron affinity (EA) of these polymers including conjugation length control, as well as the introduction of electron-donating or -withdrawing groups to the parent chromophore.

In this paper, phenoxazine ring (POZ), serves for a novel electron-donating unit. Its polymer PPOZ and the copolymer

* Corresponding author. Address: State Key Laboratory of Theoretical and Computational Chemistry, Institute of Theoretical Chemistry, Jilin University, 119 Jie Fang Road, Changchun 130023, China. Tel.: +86 431 8499856; fax: +81 431 8498026.
E-mail address: jikangf@yahoo.com (J.-K. Feng).

0032-3861/$ - see front matter © 2006 Elsevier Ltd. All rights reserved.
doi:10.1016/j.polymer.2006.02.094

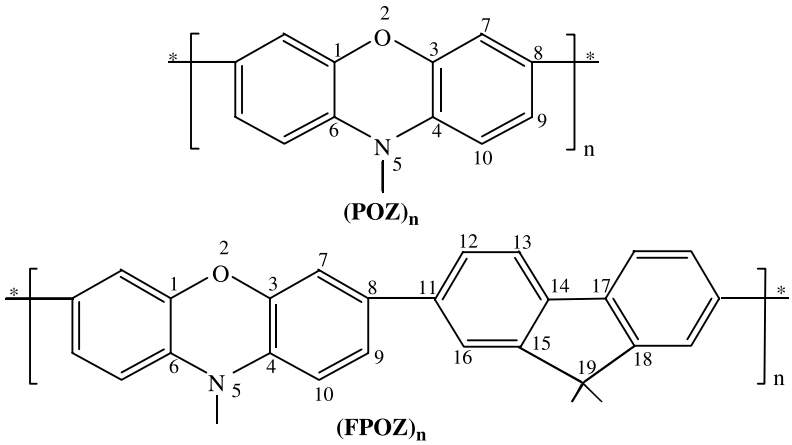

Fig. 1. The sketch map of the structures.

with fluorene (PFPOZ) have been investigated in experiment [4], which raises a way to design the copolymers with enhanced hole injection by modifying the chemical structures. Here, we further explore the ground and low-lying excited states of polymers PPOZ and PFPOZ by theoretical studies. A theoretical investigation on the IPs, EAs and band gaps of these polymers is very instrumental in guiding the experimental synthesis, which is the topic of the present work. The majority of the studies on polymers using quantum-chemistry methods consider, in fact, oligomers. The general strategy is the simulation of a number of oligomers of increasing length such that the properties of the polymers can be inferred by extrapolating the results [5]. A distinct advantage of this approach is that it can provide the convergence behavior of the structural and electronic properties of oligomers. However, the computational cost increases rapidly from monomer to oligomer, which prevents treatment of these systems using high level of theory. We were particularly interested in exploring the potential of phenoxazine as electron-donating moiety and the influence of different phenoxazine contents on electronic materials. The possible consequences of the highly non-planar structure and electron-donating property of the phenoxazine ring for the photophysics, light-emitting properties, molecular aggregation, and charge transport of π-conjugated polymers containing this ring are very intriguing to us and thus motivated our studies.

2. Computational details

All calculations on these oligomers studied in this work have been performed on the SGI origin 2000 server using Gaussian 03 program package [6]. Calculations on the electronic ground state were carried out using density functional theory (DFT), B3LYP/6-31G(d). To test electronic properties of POZ, polyfluorene [5j], which studied by our groups previously, have been employed to compare with them. The investigated polymers $(POZ)_n$ and $(FPOZ)_n$ (as depicted in Fig. 1) correspond to copolymers in literature 4, PO6 and POF2, respectively, and the main difference is that the oligomers under study substitute hexyl with methyl at 9-position in fluorene and at 10-position in phenoxazine, for the sake of reducing the time of calculation. It has been proved that the presence of alkyl groups does not significantly affect the equilibrium geometry and thus the electronic and the optical properties [7]. Then we apply the experimentally well-known reciprocal rule for polymers [5,8], which states that many properties of homopolymers tend to vary linearly as functions of reciprocal chain lengths. Selected important dihedral angles, inter-ring bond lengths and torsional angles in $(POZ)_n$ and $(FPOZ)_n$ ($n=1$–4) in the neutral ground state are listed in Table 1. The results of the optimized structures for the two series of polymeric molecules show that the bond lengths and bond angles do not suffer appreciable variation with the oligomer size in the series of $(POZ)_n$, as well as $(FPOZ)_n$. And it suggests that we can describe the basic structures of the polymers as their oligomers.

As already mentioned before, one of the most important features of the π-conjugated polymers is their ability to become highly conducting after oxidative (p-type) [9] or reductive (n-type) [10] doping. So, the cationic and anionic molecules are optimized by UB3LYP/6-31G(d) and bond lengths and dihedral angles corresponding to the ground-states are compiled in Table 2. The optimized ionic geometries were then used to calculate the ionization potential (IP) and electron affinity energies (EA).

Table 1
Selected dihedral angles, inter-ring bond distances and inter-ring torsional angles of $(POZ)_n$ and $(FPOZ)_n$ ($n=1$–4) obtained by B3LYP/6-31G(d) calculations

Dihedral angles (°)				Inter-ring distances (Å)
Oligomer	Φ(1,2,3,4)	Φ(3,4,5,6)	Inter-ring	
$(POZ)_n$				
$n=1$	22.9	22.7		
$n=2$	21.8	22.0	35.3	1.481
$n=3$	21.7	22.1	35.2	1.481
$n=4$	21.7	21.6	33.6	1.481
$(FPOZ)_n$				
$n=1$	21.3	22.1	36.3	1.482
$n=2$	21.2	21.6	36.2	1.482
$n=3$	21.4	21.1	35.9	1.482
$n=4$	21.7	21.3	35.2	1.482

Table 2
Selected dihedral angles, inter-ring bond distances and inter-ring torsional angles of $(POZ)_n$ and $(FPOZ)_n$ ($n=1$–4) in cationic and anionic states obtained by B3LYP/6-31G(d) calculations

Oligomers	Dihedral angles (°)			Inter-ring distances (Å)
	Φ(1,2,3,4)	Φ(3,4,5,6)	Inter-ring	
$(POZ)_n$				
	Cationic state			
$n=1$	5.5	8.3		
$n=2$	11.7	10.3	25.9	1.463
$n=3$	13.6	12.8	29.1	1.470
$n=4$	13.7	13.9	28.6	1.473
	Anionic state			
$n=1$	5.2	11.1		
$n=2$	15.9	17.3	6.0	1.442
$n=3$	17.2	15.8	17.1	1.459
$n=4$	17.1	15.5	22.8	1.466
$(FPOZ)_n$				
	Cationic state			
$n=1$	7.2	9.7	26.1	1.463
$n=2$	12.8	11.0	31.7	1.474
$n=3$	12.8	14.0	32.4	1.477
$n=4$				
	Anionic state			
$n=1$	16.6	19.3	14.4	1.448
$n=2$	20.0	19.3	25.5	1.468
$n=3$	19.9	19.4	28.6	1.474
$n=4$	20.2	19.8	30.3	1.476

The energy gap has been estimated from two ways, namely, HOMO–LUMO gaps (Δ_{H-L}s) and the lowest excited energies (E_gs) and the results are listed in Table 3. We employed the linear extrapolation technique in this research, which has been successfully employed to investigate several series of polymers [5c,f,j,8c,11]. The linearity between the calculated IPs, EAs, Δ_{H-L}s and E_gs of the oligomers and the reciprocal chain length is excellent for both homologous series of oligomers. The various IPs and EAs are tabulated in Table 4. The nature and the energy of 10 singlet–singlet electronic transitions have been obtained by TD-DFT/B3LYP calculations performed on the B3LYP/6-31G(d) optimized geometries, and only the most relevant singlet–singlet excited states with strong oscillator strengths ($f>0.01$) in PPOZ and PFPOZ are reported in Tables 5 and 6, respectively. The excited geometries were optimized by ab initio CIS/3-21G(d) [12]. Based on the excited geometries, the emission spectra of some of the oligomers are investigated.

Table 3
Ionization potentials, electron affinities and extraction potentials for each molecular (in eV)

(eV)	IP(v)	IP(a)	HEP	EA(v)	EA(a)	EEP
$(POZ)_n$						
$n=1$	6.42	6.24	6.13	1.49	1.33	1.19
$n=2$	5.70	5.56	5.47	0.60	0.38	0.18
$n=3$	5.40	5.30	5.21	0.26	0.09	0.05
$n=4$	5.23	5.14	5.07	0.02	0.09	0.20
$n=\infty$	4.87	4.80	4.74	0.40	0.38	0.42
Exptl.	4.8[a]					
$(FPOZ)_n$						
$n=1$	6.02	5.88	5.77	0.26	0.06	0.13
$n=2$	5.47	5.39	5.31	0.32	0.43	0.54
$n=3$	5.27	5.19	5.13	0.54	0.63	0.74
$n=4$	5.14	5.07	5.02	0.67	0.72	0.79
$n=\infty$	4.89	4.83	4.80	0.70	0.91	1.02
Exptl.	4.9[a]					

The suffixes (v) and (a) indicate vertical and adiabatic values, respectively.
[a] Ionization potential in Ref. [4].

Table 4
The HOMO–LUMO gaps (Δ_{H-L}s) by B3LYP and the lowest excitation energies (E_gs) (eV) by TDDFT of $(POZ)_n$ and $(FPOZ)_n$ ($n=1$–4)

Oligomers	Δ_{H-L}	E_g (TD)
$(POZ)_n$		
$n=1$	4.61	4.03
$n=2$	3.89	3.43
$n=3$	3.68	3.23
$n=4$	3.57	3.13
$n=\infty$	3.20	2.83
Expl.		2.44
$(FPOZ)_n$		
$n=1$	3.71	3.32
$n=2$	3.42	3.03
$n=3$	3.35	2.97
$n=4$	3.30	2.92
$n=\infty$	3.16	2.78
Expl.		2.61

3. Results and discussion

3.1. Ground states structural properties

From Table 1, we notice that the POZ moiety exhibits high-non-planar conformation (as depicted in Fig. 2) and its structure tend to be bending in the butterflylike shape across the line fixed by the oxygen and nitrogen atoms with the average values of dihedral angles Φ(1,2,3,4) and Φ(3,4,5,6) in the oligomers of PPOZ around 21 and 22°, respectively, and that suggests small molecular orbital overlap between the oxygen or nitrogen and the joint atoms. In PPOZ, one POZ ring is twisted by about 35° relative to the adjacent POZ ring. On the contrary, because the dihedral angle between two phenyl rings in fluorene segment of the oligomers in PFPOZ is fixed by ring bridged-atoms, which tend to keep their normal tetrahedral angles in their ring linkage and to keep their quasi planar conformations. The torsional angels between the two adjacent fluorene and POZ units are around 35°.

3.2. Frontier molecular orbitals

Fig. 3 describes the evolution of the B3LYP/6-31G(d) calculated highest occupied molecular orbital (HOMO) and lowest unoccupied molecular orbital (LUMO) energies as a function of the inverse number of monomer units in $(POZ)_n$ and $(FPOZ)_n$. For the sake of comparison, the frontier energy levels of $(F)_n$ [5j] ($n=1$–4) are also listed in Fig. 3. As is usual in π-conjugated systems, the energy of the frontier electronic levels evolves linearly with inverse chain length in the four systems: the HOMO energies increase, whereas the LUMO energies decrease [13]. Similar energies are obtained for the

Table 5
Electronic transition data obtained by the TDDFT/B3LYP/6-31G(d) for $(POZ)_n$

Electronic transitions	Wavelengths (nm)	f	MO/character	Coefficient
POZ				
$S_1 \leftarrow S_0$	307.82	0.0219	HOMO→LUMO	0.65
$S_2 \leftarrow S_0$	285.73	0.1537	HOMO→LUMO+1	0.61
$S_4 \leftarrow S_0$	227.81	0.0811	HOMO→LUMO+3	0.59
			HOMO-2→LUMO	0.35
$S_5 \leftarrow S_0$	216.33	0.5848	HOMO→LUMO+4	0.63
$S_8 \leftarrow S_0$	194.61	0.0254	HOMO-1→LUMO+1	0.52
			HOMO-1→LUMO+4	0.45
$(POZ)_2$				
$S_1 \leftarrow S_0$	361.64	0.5097	HOMO→LUMO	0.66
$S_4 \leftarrow S_0$	306.50	0.2186	HOMO→LUMO+2	0.62
$S_5 \leftarrow S_0$	293.15	0.0219	HOMO→LUMO+3	0.64
$S_6 \leftarrow S_0$	290.69	0.0182	HOMO→LUMO+4	0.64
$S_8 \leftarrow S_0$	283.42	0.0685	HOMO-1→LUMO+2	0.60
$(POZ)_3$				
$S_1 \leftarrow S_0$	383.56	0.8162	HOMO→LUMO	0.66
$S_2 \leftarrow S_0$	346.75	0.1095	HOMO-1→LUMO	0.60
			HOMO→LUMO+1	0.22
$S_3 \leftarrow S_0$			HOMO-2→LUMO	0.52
			HOMO-1→LUMO+1	0.35
$S_4 \leftarrow S_0$			HOMO→LUMO+1	0.62
$S_5 \leftarrow S_0$			HOMO→LUMO+2	0.57
			HOMO-2→LUMO	0.30
$(POZ)_4$				
$S_1 \leftarrow S_0$	395.85	1.2980	HOMO→LUMO	0.65
$S_4 \leftarrow S_0$	344.56	0.1602	HOMO-2→LUMO	0.50
			HOMO-1→LUMO+1	0.34
$S_6 \leftarrow S_0$	332.01	0.1075	HOMO-1→LUMO+1	0.49
			HOMO-2→LUMO	0.40
$S_7 \leftarrow S_0$	323.73	0.0132	HOMO→LUMO+2	0.58
			HOMO-1→LUMO+1	0.25
Experiment	397[a]	424[b]		

[a] Measured in dilute solution.
[b] Measured for thin films on fused quartz plates in Ref. [4].

LUMO of the longest oligomers of PFPOZ (∼ −1.3 eV) and PF (∼ −1.4 eV) [5j], indicating that the electron-accepting ability of copolymer PFPOZ does not worsen. Turning to the evolution of the HOMO levels, the observed 0.14 eV difference of HOMO in PFPOZ between the monomer and quadmer is rather small compared to other monomer/quadmer systems such as thiophene-based (0.44 eV) [5i] and fluorene (0.63 eV) [5j] systems. The main reason is that electronic delocalization is limited by the non-planar geometry of the phenoxazine ring. Most importantly, the HOMO of PPOZ (−4.4 eV) and PFPOZ (∼ −4.6 eV) dramatically increase by about 0.8 and 0.6 eV with respective to PF (∼ −5.2 eV) [5j], indicating that the electron-donating POZ units significantly improve the hole-accepting properties and result in more efficient charge carrier balance.

The results of Fig. 3 can be easily rationalized by analyzing how the nature of the frontier electronic levels of the fluorene chains is affected by the incorporation of POZ unit (Fig. 4). In FPOZ, the HOMO remains localized on POZ and less on fluorene; the shapes of the LUMOs become drastically different, being mainly localized on the fluorene unit in the copolymer. This charge transfer implies the POZ serves as electron-donating functionalities by the presence of the electron-rich oxygen and nitrogen heteroatoms. It is also the reason why the HOMO levels of PFPOZ are close to that of PPOZ, whereas the LUMO levels are similar with PF. Furthermore, in FPOZ, the HOMO possesses an antibonding character between the subunits. On the other hand, the LUMO of all the oligomers generally shows a bonding character between the subunits. This is rationalized by the fact that the energy separation between the HOMO of F and POZ monomer is large (0.98 eV) and leads to weak interactions between the two building blocks; in contrast, the separation between the corresponding HOMO levels is smaller (0.60 eV) and promotes stronger interactions between the two units, thus giving rise to a delocalized LUMO level in the FPOZ monomer. In fact, the frontier orbitals in all the oligomers of both series exhibit the similar character with the monomer as shown in Fig. 5.

3.2.1. The geometry in the cationic and anionic states

Comparing the results in Tables 1 and 2, we can find the structural variation in cationic and anionic states relative to the neutral ground states. One can see that the inter-ring distances between the two adjacent subunits decrease in the both cationic and anionic states in the oligomers of $(POZ)_n$, as well as the

Table 6
Electronic transition data obtained by the TDDFT//B3LYP/6-31G(d) for $(FPOZ)_n$

Electronic transitions	Wavelengths (nm)	f	MO/character	Coefficient
POZ				
$S_1 \leftarrow S_0$	373.77	0.4354	HOMO→LUMO	0.67
$S_2 \leftarrow S_0$	311.37	0.0393	HOMO→LUMO+2	0.65
$S_3 \leftarrow S_0$	304.19	0.0131	HOMO→LUMO+1	0.66
$S_4 \leftarrow S_0$	292.55	0.1630	HOMO→LUMO+3	0.60
$S_5 \leftarrow S_0$	286.07	0.3681	HOMO→LUMO+4	0.46
			HOMO-1→LUMO	0.42
$S_6 \leftarrow S_0$	283.52	0.3971	HOMO-1→LUMO	0.46
			HOMO→LUMO+4	0.44
$S_8 \leftarrow S_0$	262.54	0.0141	HOMO-1→LUMO+1	0.55
			HOMO-4→LUMO	0.38
$(FPOZ)_2$				
$S_1 \leftarrow S_0$	409.47	1.0825	HOMO→LUMO	0.65
$S_2 \leftarrow S_0$	383.02	0.1753	HOMO-1→LUMO	0.62
$S_3 \leftarrow S_0$	366.44	0.1406	HOMO→LUMO+1	0.63
$S_4 \leftarrow S_0$	347.37	0.0550	HOMO-1→LUMO+1	0.64
$S_5 \leftarrow S_0$	319.28	0.0187	HOMO→LUMO+2	0.55
			HOMO-1→LUMO+5	0.23
$(FPOZ)_3$				
$S_1 \leftarrow S_0$	417.21	1.7347	HOMO→LUMO	0.64
$S_2 \leftarrow S_0$	397.99	0.1378	HOMO-1→LUMO	0.51
			HOMO→LUMO+1	0.33
$S_3 \leftarrow S_0$	382.99	0.2715	HOMO-2→LUMO	0.49
			HOMO-1→LUMO+1	0.32
$S_4 \leftarrow S_0$	377.90	0.0188	HOMO→LUMO+1	0.52
			HOMO-1→LUMO	0.37
$S_5 \leftarrow S_0$	367.23	0.1598	HOMO-1→LUMO+1	0.41
			HOMO-2→LUMO	0.33
$(FPOZ)_4$				
$S_1 \leftarrow S_0$	424.44	2.2412	HOMO→LUMO	0.60
$S_2 \leftarrow S_0$	409.55	0.0759	HOMO-1→LUMO	0.48
			HOMO→LUMO+1	0.41
$S_3 \leftarrow S_0$	395.77	0.3872	HOMO-2→LUMO+1	0.40
			HOMO-1→LUMO+1	0.33
$S_4 \leftarrow S_0$	386.35	0.0375	HOMO→LUMO+1	0.49
			HOMO-1→LUMO	0.38
$S_5 \leftarrow S_0$	383.06	0.2915	HOMO-3→LUMO	0.37
			HOMO-2→LUMO+1	0.34
Experiment	417[a]	417[b]		

[a] Measured in dilute solution.
[b] Measured for thin films on fused quartz plates Ref. [4].

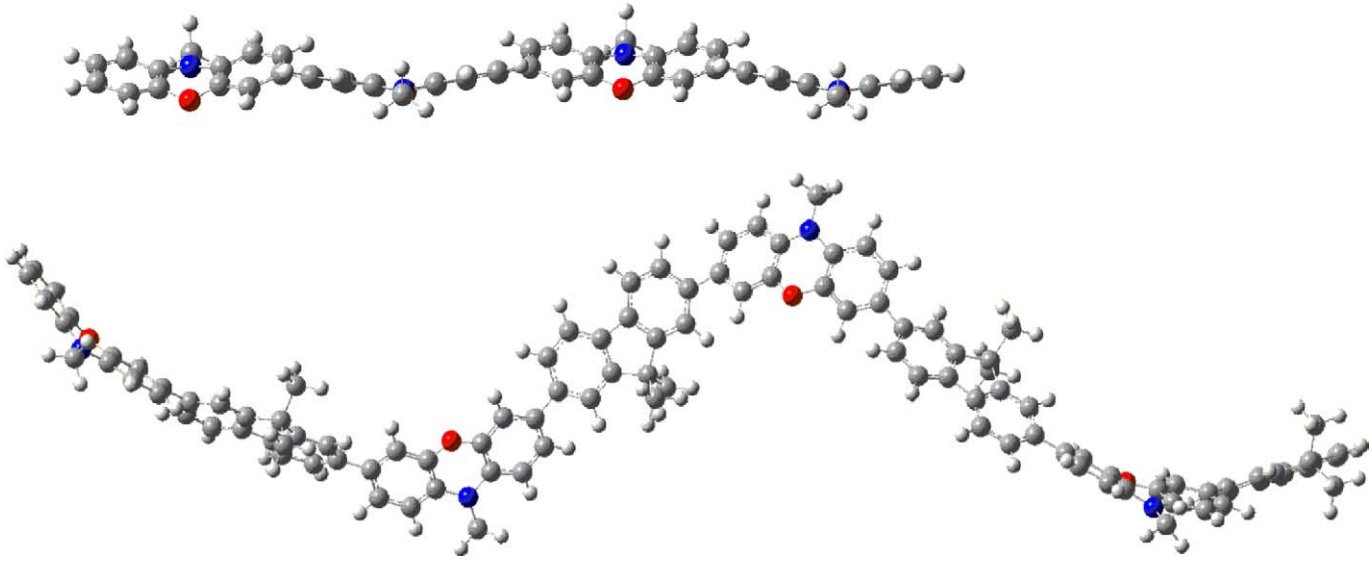

Fig. 2. Optimized structures of (POZ) (up) and (FPOZ) (down).

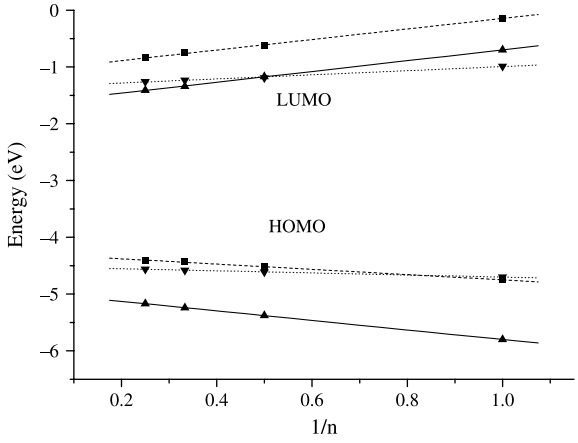

Fig. 3. B3LYP/6-31G(d) calculated HOMO and LUMO energies of PPOZ (dashed lines), PFPOZ (dotted lines) and PF (solid lines) oligomers as a function of the inverse number of monomer units.

series of $(FPOZ)_n$. The shortening of the inter-ring distances in ionic states relative to that in neutral state can easily be seen from the HOMO and LUMO characters plotted in Fig. 5. There is antibonding between the inter-ring bridge atoms in the HOMO. Hence, removing an electron from HOMO leads to a shortening of the inter-ring distances in cationic state relative to the neutral state. On the other hand, the LUMO of all the oligomers generally shows a bonding character between the subunits. The shortening of the inter-ring distance in the anionic state is due to the bonding interactions between the π-orbitals on the two adjacent moieties.

On the other hand, the injection of electrons or holes in these oligomers of both series induces to the better conjugations and the whole molecules tend to more planar than their corresponding neutral ground states. In the cationic state of both series of PPOZ and PFPOZ, the torsional angles, Φ(1,2,3,4) and Φ(3,4,5,6) of POZ rings are even smaller than that in their anionic state. This is because the HOMO orbitals are mainly localized on POZ rings, whereas the LUMO orbitals are predominant π-bonding

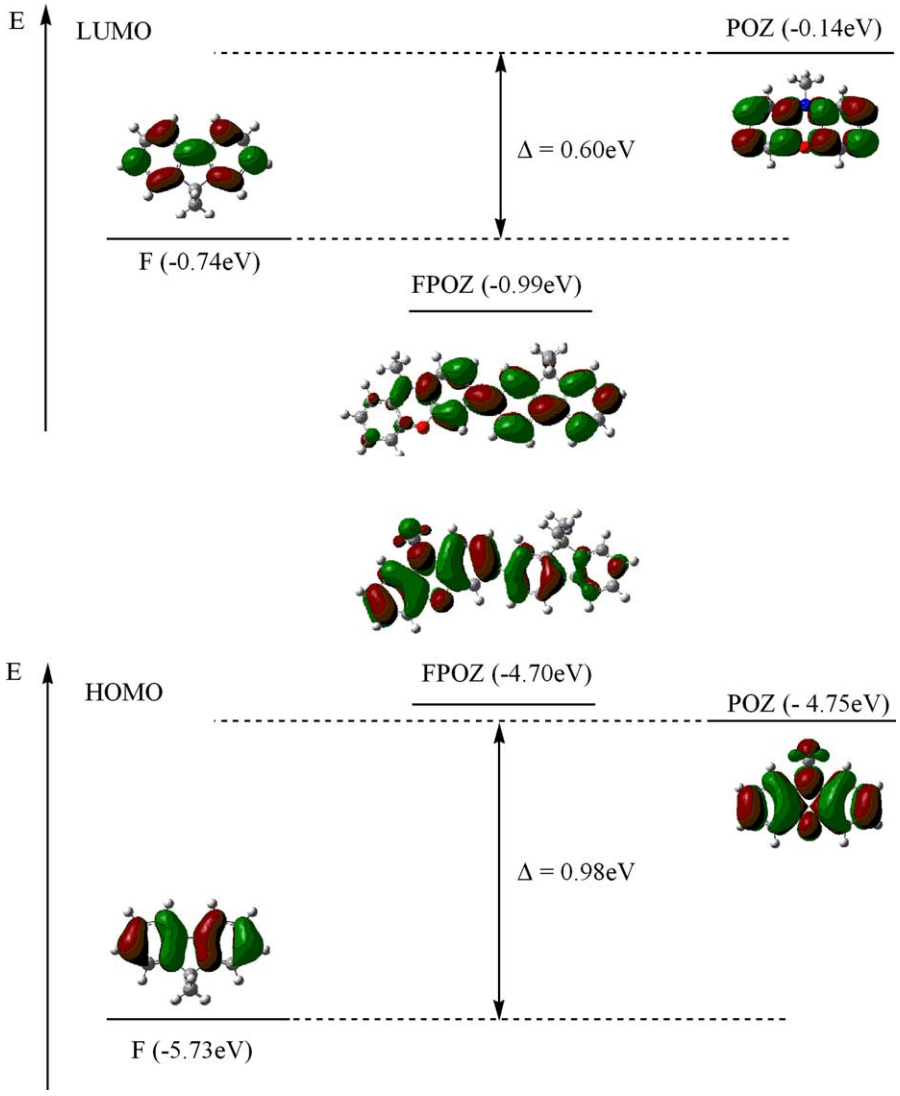

Fig. 4. Energies and shapes of the HOMO (top) and LUMO (bottom) orbitals of fluorene (F), phenoxazine (POZ) and FPOZ, as calculated at B3LYP/6-31G(d) level.

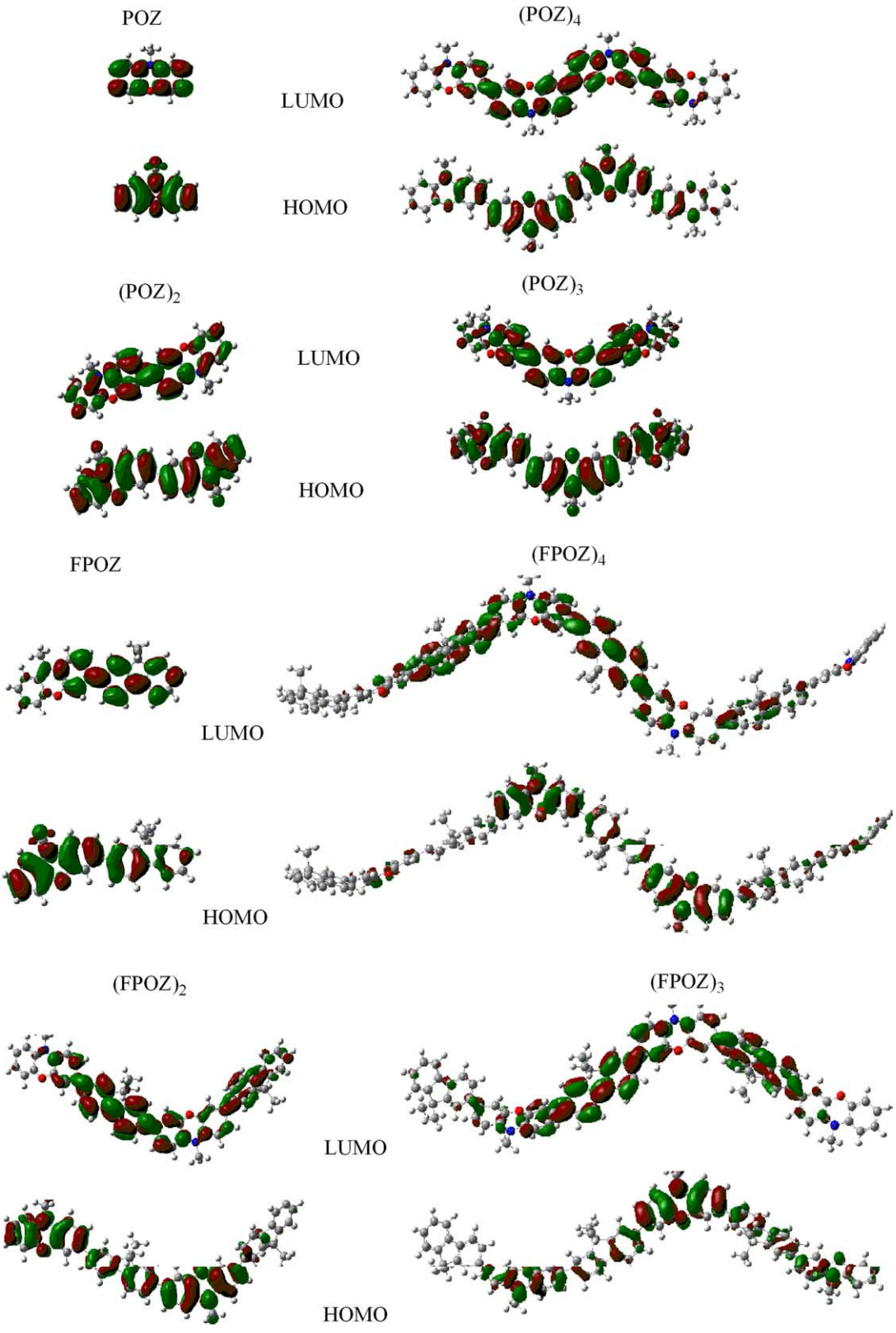

Fig. 5. B3LYP/6-31G(d) electronic density contours of the frontier orbitals for $(POZ)_n$ and $(FPOZ)_n$ ($n = 1$–4).

character of fluorene rings, the injection of a hole has much effects on HOMO and thus on the structure of POZ. However, as for the inter-ring dihedral angles, they twist less in the anionic states than that in their cationic states. Indeed, the injection of an electron should enhance the bonding character of LUMO and thus enhance the electronic conjugation over the whole molecular structure in the anionic states.

3.2.2. Ionization potentials and electron affinities

The adequate and balanced transport of both injected electrons and holes are important in optimizing the performance of OLED devices. The ionization potential (IPs) and electron affinity (EAs) are calculated by DFT to estimate the energy barrier for the injection of both holes and electrons into the polymer. Table 3 contains the ionization potentials (IPs), electron affinities (EAs), both vertical (v; at the geometry of the neutral molecule) and adiabatic (a; optimized structure for both the neutral and charged molecule), and extraction potentials (HEP and EEP for the hole and electron, respectively) that refer to the geometry of the ions [14]. The IPs, EAs, HEPs and EEPs for infinite chains of the polymers were determined by plotting these values of oligomers against the reciprocal of the number of modeling polymeric units and by extrapolating the number of units to infinity. It can be seen from Table 3 that the ionization potentials (IP) of PPOZ and PFPOZ based on the empirical formula $IP = E_{ox}^{onset} + 4.4\,eV$ are estimated to be 4.8 and 4.9 eV, respectively [4], which agree well with our extrapolated IPs with the average values of 4.80 and 4.84 eV.

One general challenge for the application of polyfluorenes in PLEDs is achievement of low-ionization potential (p-type) conjugated polymers for better hole injection/transport in polymer electronic devices. For PPOZ and PFPOZ, the energies required to create a hole in the polymers are around 4.80 and 4.84 eV, respectively, which are both lower than that in PF (5.4 eV) [5j]. Thus, hole injection and transportation from PPOZ to the copolymer PFPOZ are expected to be easier than to the PF, and as a consequence the charge carrier balance is better in the devices constructed from the copolymers.

3.3. HOMO–LUMO gaps and the lowest excitation energies

There are two theoretical approaches for evaluating the energy gap in this paper. One way is based on the ground-state properties, from which the band gap is estimated from the energy difference between the highest occupied molecular orbital (HOMO) and the lowest unoccupied molecular orbital (LUMO) [15], when $n = \infty$, termed the HOMO–LUMO gaps (Δ_{H-L}s). The TDDFT, which has been used to study systems of increasing complexity due to its relatively low-computational cost and also to include in its formalism the electron correlation effects, is also employed to extrapolate energy gap of polymers from the calculated first dipole-allowed excitation energy of their oligomers.

Here, the HOMO–LUMO gaps (Δ_{H-L}s) and lowest singlet excited energies (E_g) are both listed in Table 4 and the relationships between the calculated Δ_{H-L} and the E_g and the inverse chain length are plotted in Fig. 6. There is a good linear relation between the energy gaps by both methods and the inverse chain length. Obviously, the E_g presented in Table 4 yields a better agreement with the experimental data than Δ_{H-L} in this study. However, there are still errors between the calculated results and the experimental values from the edge of the electronic band. One factor responsible for deviations by both methods from experimental is that the predicted band gaps are for the isolated gas-phase chains, while the experimental band gaps are measured in the liquid phase where the environmental influence may be involved. Additionally, it should be borne in mind that solid-state effects (like polarization effects and intermolecular packing forces) have been neglected in the calculations. The latter can be expected to result in a decreased inter-ring twist and consequently a reduced gap in a thin film compared to an isolated molecule as considered in the calculations [16].

The band gaps obtained by HOMO–LUMO gaps and TD-DFT are 3.33 and 2.91 eV for PF [5j], respectively, which are both higher than that of PPOZ and PFPOZ with the same corresponding methods, indicating the reduced band gaps of fluorene-based copolymers due to the highly non-planar structure of POZ. So we can estimate that the narrower band gaps of both PPOZ and PFPOZ would lead to the red-shifted absorption and emission wavelengths.

3.4. Absorption spectra

As shown in Tables 5 and 6, three interesting trends can be observed in both series of oligomers: (1) in the considerable broad regions, the electronic states exhibit large f values with

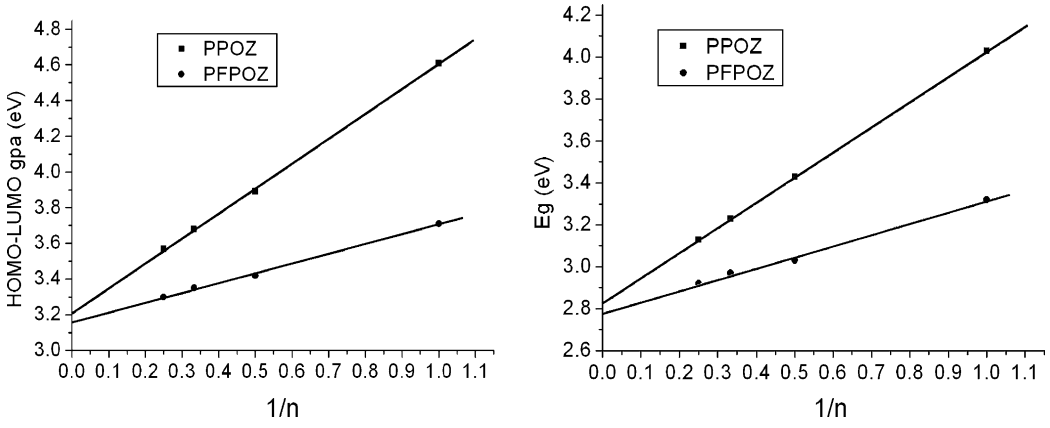

Fig. 6. The HOMO–LUMO gaps by B3LYP and the lowest excitation energies E_gs by TD-DFT as a function of reciprocal chain length n in oligomers of $(POZ)_n$ and $(FPOZ)_n$.

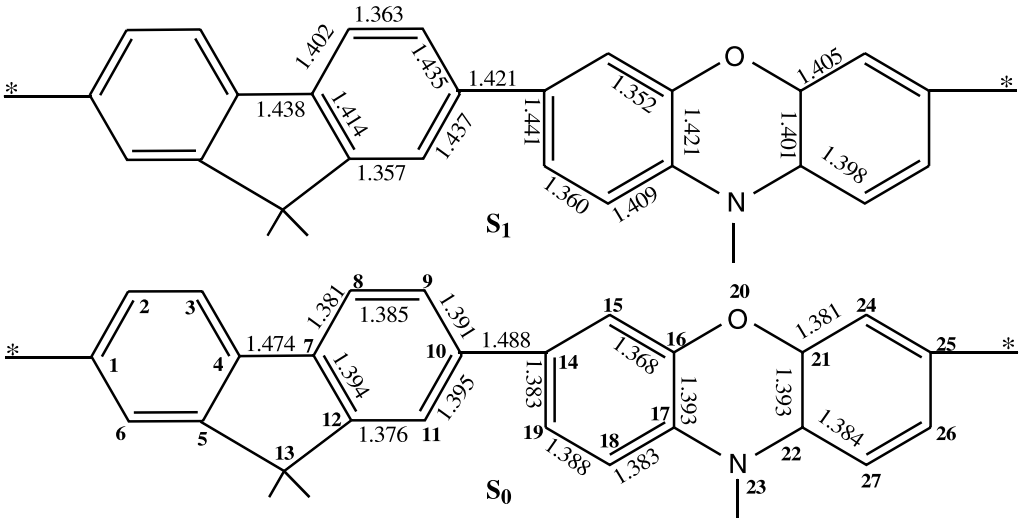

Fig. 7. Comparison of the excited structure (S_1) by CIS/3-21G(d) with the ground geometry (S_0) by HF/3-21G(d) of FPOZ.

no clear peak; (2) the oscillator strengths (*f*) of the lowest $S_0 \rightarrow S_1$ electronic transition are the largest in both series of oligomers, except for the monomer of PPOZ; (3) the oscillator strength coupling the lowest CT π–π^* singlet excited state increase strongly when going from an isolated molecule to a molecular group and this trend goes along with the conjugation lengths increasing.

All electronic transitions are of the $\pi\pi^*$ type and no localized electronic transitions are exhibited among the calculated singlet–singlet transitions. Excitation to the S_1 state corresponds almost exclusively to the promotion of an electron from the HOMO to the LUMO (except for POZ). As in the case of the oscillator strength, the absorption wavelengths arising from $S_0 \rightarrow S_1$ electronic transition increase progressively with the conjugation lengths increasing. It is reasonable, since HOMO $\rightarrow$ LUMO transition is predominant in $S_0 \rightarrow S_1$ electronic transition and as analysis above that with the extending molecular size, the HOMO–LUMO gaps decrease.

As shown in Table 5, each oligomer of PPOZ has a rather broad absorption with no clear peak in nearly 60 nm regions. Taken $(POZ)_4$ as an example whose character is relative close to the polymer, it has a strong absorption in the 395–323 nm range with absorption maxima at around 395 and 344 nm, respectively. In the case of the phenoxazine–fluorene alternating copolymer, $(FPOZ)_4$, it exhibits maximum UV–vis absorption at around 424 and 395 nm. The related polyfluorene homopolymer has an intense structureless absorption center at 370 nm. These results show that the ground-state electronic structure of the alternating copolymer PFPOZ is completely different from those of the related homopolymers by the presence of the highly non-planar POZ moiety. It can be seen that the UV–vis absorption spectrum of PFPOZ exhibited red-shifted from that of the PPOZ, in agreement with the energy gaps determined from the absorption onset. Compared with PF ($\sim$368 nm by TDDFT) [5j], the absorption spectra exhibit bathochromic shift in PFPOZ by the introduction of electron-donating group POZ.

3.5. The properties of excited structures and the emission spectra

Up to now, the standard for calculating excited state equilibrium properties of larger molecules is the configuration interaction singles (CIS) method. In this study, we hope to investigate the excited state properties by this method, in despite of not accurate. Because the calculation of excited-state properties typically requires significantly more computational effort than is needed for the ground states and dramatically constrains by the size of the molecules, we only optimize the monomer and dimer of PPOZ and monomer of PFPOZ by CIS/3-21G(d). In Fig. 7 we take FPOZ as an example to compare the excited structures of PFPOZ by CIS/3-21G(d) with their ground structures by HF/3-21G(d). Interestingly, the main characters of the front orbitals by HF/3-21G(d) are the same to that by B3LYP/6-31G(d). As shown, some of the bond lengths lengthened, but some shortened. We can predict the differences of the bond lengths between the ground (S_0) and singlet excited state (S_1) from MO nodal patterns. Due to the singlet state corresponds to an excitation from the HOMO to the LUMO in all considered oligomers, we can explore the bond lengths variation by analyzing the HOMO and LUMO. The HOMO is bonding across r(7,8), r(7,12), r(9,10) r(10,11), r(14,19), r(16,17), r(17,18), r(21,24) and r(22,27) bonds in FPOZ, but the LUMO has nodes in these regions. Therefore one would expect elongation of these bonds; the data in the Fig. 7 shows that these bonds are in fact considerably longer in the excited state. The HOMO has a node across the r(4,7), r(8,9), r(11,12), r(10,14), r(15,16) and r(18,19) bonds in FPOZ, while the LUMO is bonding. The data confirm the anticipated contraction of these bonds.

The dihedral angles Φ(16,20,21,22) and Φ(17,23,22,21) in POZ, $(POZ)_2$ and FPOZ reduced from 16 and 17° by HF/3-21G(d) to nearly 7 and 9° by CIS/3-21G(d), respectively. The bridge bonds between each conjugation segment rotate to some extent when excited from ground to excited states. The inter-ring torsional angles in $(POZ)_2$ and FPOZ decrease from 47 and

Table 7
Electronic transition data obtained by the TDDFT/B3LYP/3-21G(d) based on the CIS/3-21G(d) geometries for the monomer and dimer of PPOZ and monomer of PFPOZ

Electronic transition	Wavelengths (nm)	f	MO/character	Coefficient	Stokes shift (eV)	Wavelengths exp. (nm)	
POz $S_1 \rightarrow S_0$	373.62	0.0150	HOMO → LUMO	0.67	0.70		
$(POz)_2$ $S_1 \rightarrow S_0$	422.48	0.7381	HOMO → LUMO	0.65	0.50	458[a]	473[b]
FPOZ $S_1 \rightarrow S_0$	432.19	0.6375	HOMO → LUMO	0.64	0.55	462[a]	475[b]

[a] Normalized PL emission spectra in 10^{-5} M tolurene solutions.
[b] Thin film on silica substrates in Ref. [4].

49° to 1 and 2°, respectively. It is obvious that the excited structure has a strong coplanar tendency in both the series, that is, the conjugation is better in the excited structure, which further approves the predictions from frontier orbitals.

Consequently, the emission calculations are made by reoptimizations of the POZ, $(POZ)_2$ and FPOZ with the CIS/3-21G(d) method in their first singlet excited states, followed by using the resulting geometries to perform TD calculations employing the B3LYP/3-21G(d) method and the results are tabulated in Table 7. Although there are some discrepancies between the calculated values and the observed data, they have the same trend that the emission peaks exhibit slight bathochromic shift in FPOZ compared with $(POZ)_2$, due to different POZ fractions. The fluorescent peaks all arise from $S_1 \rightarrow S_0 \pi\pi^*$ electron transition dominated by HOMO → LUMO.

In addition, as shown in Table 7, the observed rather large Stokes shift in these oligomers must thus be explained by an alternative mechanism. We note that the phenoxazine ring is highly non-planar in the ground state, impeding sufficiently π-stacking aggregation and intermolecular excimer formation. On the other hand, we observe that the phenoxazine ring and even the whole molecular structures of PPOZ and PFPOZ in the excited state are more planar than that in the ground state. Consequently, the relaxed singlet excited state from which emission occurs is lower lying than if photoinduced planarization were absent.

4. Conclusion

The presence of the electron-rich oxygen and nitrogen heteroatoms results in the highly non-planar conformations in phenoxazine ring relative to the rigid planar structures in fluorene ring. The highly non-planar structural properties in the homopolymer PPOZ and alternating copolymer PFPOZ impede π-stacking aggregation and intermolecular excimer formation, resulting in identical dilute solution and solid-state photophysics, which hampers the application of polyfluorenes in PLEDs. All decisive molecular orbitals are delocalized on all subunits of the oligomers. The HOMO possesses an antibonding character between subunits, which may explain the non-planarity observed for these oligomers in their ground state. On the other hand, the LUMO shows bonding character between the two adjacent rings, in agreement with the more planar S_1 excited state. Importantly, electron-donating groups POZ not only enhance the optical stability and thus increase fluorescence quantum yields, but also improve the hole injection and efficient charge carrier balance due to the higher HOMO levels and the lower IPs, compared with those of conventional polyfluorene materials. These two points are both essential for light-emitting polymers, and provide the opportunity of tuning the electronic and optical properties of the resulting polymers.

Our calculated results also indicate that the incorporation with POZ will reduce the band gaps of fluorene-based copolymers due to the highly non-planar structure, and with the fractions of the POZ increasing, the band gaps also increase. Both PPOZ and PFPOZ have rather broad absorption bands and have two absorption maximum, which is completely different from those of the related fluorene polymers. The absorption and emission spectra of $(FPOZ)_n$ exhibit red-shifted compared with $(POZ)_n$ ascribed to the different POZ fractions and the two series both emit a blue light.

Finally, this theoretical study confirmed experimental results where it was shown that by modification of chemical structures could greatly modulate and improve the electronic and optical properties of pristine polymers. Furthermore, using theoretical methodologies, we showed that is possible to predict reasonably the electronic properties of conjugated systems and we are convinced that the systematic use of those theoretical tools should contribute to orientate the synthesis efforts and help understand the structure–properties relation of these conjugated materials.

Acknowledgements

This work is supported by the Major State Basis Research Development Program (No. 2002CB 613406).

References

[1] (a) Skotheim TA, Elsenbaumer RL, Reynolds JR, editors. Handbook of conducting polymers. 2nd ed. New York: Marcel Deker; 1998.
(b) Bernier P, Lefrant S, Bidan G, editors. Advances in synthetic metals: twenty years of progress in science and technology. Lausanne: Elsevier; 1999.
(c) Leclerc M, Faïd K. Adv Mater 1997;9:1087.
(d) Leclerc M. J Polym Sci, Polym Chem 2001;39:2867.
[2] (a) Burn PL, Holmes AB, Kraft A, Bradley DDC, Brown AR, Friend RH, et al. Nature 1992;356:47.
(b) Kraft A, Grimsdale AC, Holmes AB. Angew Chem, Int Ed 1998;37:402.
[3] (a) Neher D. Macromol Rapid Commun 2001;22:1356.

(b) Cho NS, Hwang DH, Lee JI, Jung BJ, Shim HK. Macromolecules 2002;35:1224.
(c) Ego C, Marsitzky D, Silva C, Friend RH. J Am Chem Soc 2003;125:437.
[4] Zhu Y, Babel A, Jenekhe SA. Macromolecules 2005;38(19):7983–91.
[5] (a) Zhang JP, Frenking G. J Phys Chem A 2004;108:10296–301.
(b) Briére JF, Côté M. J Phys Chem B 2004;108:3123–9.
(c) Ford WK, Duke CB, Paton A. J Chem Phys 1982;77(9):4564–72.
(d) Klaerner G, Miller RD. Macromolecules 1998;31:2007–9.
(e) Brédas JL, Chance RR, Silbey R. Phys Rev B 1982;26:5843–54.
(f) Ma J, Li SH, Jiang YS. Macromolecules 2002;35:1109–15.
(g) Zhang GL, Ma J, Jiang YS. Macromolecules 2003;36:2130–40.
(h) Cao H, Ma J, Zhang GL, Jiang YS. Macromolecules 2005;38:1123–30.
(i) Zhou X, Ren AM, Feng JK. Polymer 2004;7747–57.
(j) Wang JF, Feng JK, Ren AM, Liu XD, Ma YG, Lu P, et al. Macromolecules 2004;37:3451.
[6] Frisch MJ, Trucks GW, Schiegel HB, Scuseria GE, Robb MA, Cheeseman JR, et al. Gaussian 03. Revision B.04. Pittsburgh, PA: Gaussian, Inc.; 2003.
[7] (a) Foresman JB, Head-Gordon M, Pople JA. J Phys Chem 1992;96:135.
(b) Belletête M, Beaypré S, Bouchard J, Blondin P, Leclerc M, Durocher G. J Phys Chem 2000;104:9118.
[8] (a) Gao Y, Liu C, Jiang Y. J Phys Chem A 2002;106:5380.
(b) Cornil J, Gueli I, Dkhissi A, Sancho-Garcia JC, Hennebicq E, Calbert JP, et al. J Chem Phys 2003;118:6615–23.
(c) Ford WK, Duke CB, Salaneck WR. J Chem Phys 1982;77:5030.
[9] Agrawal AK, Jenekhe SA. Chem Mater 1996;8:579.
[10] Ho PKH, Kim J-S, Burroughes JH, Becker H, Lis SFY, Brown TM, et al. Nature 2000;404:481.
[11] Brédas JL, Silbey R, Boudreaux DS, Chance RR. J Am Chem Soc 1983;105:6555.
[12] (a) Yang L, Ren AM, Feng JK, Liu XD, Ma YG, Zhang HX. Inorg Chem 2004;43:5961.
(b) Yang L, Ren AM, Feng JK, Ma YG, Zhang M, Liu XD, Shen JC, Zhang HX. J Phys Chem 2004;108:6797.
(c) Yang L, Ren AM, Feng JK. J Comput Chem 2005;26:969.
[13] Cornil J, Gueli I, Dkhissi A, Sancho-Garcia JC, Hennebicq E, Calbert JP, et al. J Chem Phys 2003;118:6615–23.
[14] (a) Curioni A, Boero M, Andreoni W. Chem Phys Lett 1998;294:263–71.
(b) Irene W, Estelle BA, Olivier S, Alain I, Patrice LB. J Opt A: Pure Appl Opt 2002;4:S258–S60.
[15] (a) Hay PJ. J Phys Chem A 2002;106:1634–41.
(b) Curioni A, Andreoni W, Treusch R, Himpsel FJ, Haskal E, Seidler P, et al. J Appl Phys Lett 1998;72:1575–7.
(c) Hong SY, Kim DY, Kim CY, Hoffmann R. Macromolecules 2001;34:6474–81.
[16] (a) Puschning P, Ambrosch-Draxl C, Heimel G, Zojer E, Reset R, Leising G, et al. Synth Met 2001;116:327.
(b) Eaton VJ, Steele D. J Chem Soc: Faraday Trans 2 1973;2:1601.